Late-onset enteric virus infection associated with hepatitis (EVAH) in transplanted SCID patients

Quentin Riller, Jacques Fourgeaud, Julie Bruneau, Suk See de Ravin, Grace Smith, Mathieu Fusaro, Samy Meriem, Aude Magerus, Marine Luka, Ghaith Abdessalem, et al.

HHS Public Access

Author manuscript

J Allergy Clin Immunol. Author manuscript; available in PMC 2023 December 01.

Published in final edited form as:

J Allergy Clin Immunol. 2023 June ; 151(6): 1634–1645. doi:10.1016/j.jaci.2022.12.822.

Late-onset enteric virus infection associated with hepatitis (EVAH) in transplanted SCID patients

A full list of authors and affiliations appears at the end of the article.

Abstract

Background: Allogenic hematopoietic stem cell transplantation (HSCT) and gene therapy (GT) are potentially curative treatments for severe combined immunodeficiency (SCID). Late-onset posttreatment manifestations (such as persistent hepatitis) are not uncommon.

Objective: We sought to characterize the prevalence and pathophysiology of persistent hepatitis in transplanted SCID patients (SCIDH+) and to evaluate risk factors and treatments.

Methods: We used various techniques (including pathology assessments, metagenomics, single-cell transcriptomics, and cytometry by time of flight) to perform an in-depth study of different tissues from patients in the SCIDH+ group and corresponding asymptomatic similarly transplanted SCID patients without hepatitis (SCIDH−).

Results: Eleven patients developed persistent hepatitis (median of 6 years after HSCT or GT). This condition was associated with the chronic detection of enteric viruses (human Aichi virus, norovirus, and sapovirus) in liver and/or stools, which were not found in stools from the SCIDH− group (n = 12). Multiomics analysis identified an expansion of effector memory $CD8^+$ T cells with high type I and II interferon signatures. Hepatitis was associated with absence of myeloablation during conditioning, split chimerism, and defective B-cell function, representing 25% of the 44 patients with SCID having these characteristics. Partially myeloablative retransplantation or GT of patients with this condition (which we have named as “enteric virus infection associated with hepatitis”) led to the reconstitution of T- and B-cell immunity and remission of hepatitis in 5 patients, concomitantly with viral clearance.

Conclusions: Enteric virus infection associated with hepatitis is related to chronic enteric viral infection and immune dysregulation and is an important risk for transplanted SCID patients with defective B-cell function.

Graphical Abstract

Corresponding author: Bénédicte Neven, MD, PhD, Necker-Children’s Hospital, 149 rue de Sèvres, 75015, Paris, France. benedicte.neven@aphp.fr.

*Co-first authors.

‡These authors contributed equally to this work.

§Co-senior authors.

Disclosure of potential conflict of interest: The authors declare that they have no relevant conflicts of interest.

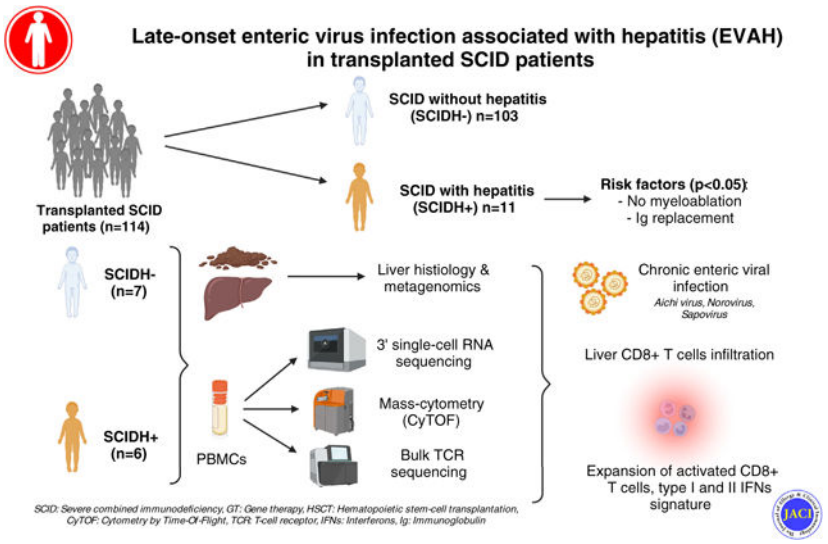

Keywords

SCID; enteric virus; CD8$^+$ T cells; interferon; B-cell function; transplantation; gene therapy

Severe combined immunodeficiencies (SCIDs) are a group of genetically defined, inborn errors of immunity characterized by an early block in T-cell differentiation and thus profound T-cell lymphopenia. Depending on the underlying genetic defect, natural killer(NK) cellsmay be lackingand B cellsmaybe nonfunctional or absent. SCID is life-threatening from birth onward because of a greater risk of infections. Allogenic hematopoietic stem cell transplantation (HSCT) is a potentially curative treatment for SCID,[1,2] and gene therapy (GT) with genetically modified autologous hematopoietic stem cells is a treatment option in some patients.[3,4] Insome circumstances, HSCT or GT without myeloablation is feasible because (1) the absence of recipient T cells and (in some cases) NK cells significantly reduces the risk of rejection and (2) donor progenitor cells have a selective advantage for engagement toward T-celldifferentiation. However, B-celldysfunction often persists after nonmyeloablative HSCT or GT, and T-cell reconstitution can be suboptimal or may decline over time.[5,6]

Since the first HSCT performed in 1968,[7] overall survival rates have improved remarkably and now range from 70% to 90% depending primarily on donor compatibility and the recipient's clinical status.[5,8,9] Therefore, the long-term function and stability of immune reconstitution and the latter's relationship with the patient's quality of life have become issues of the utmost importance. For example, follow-up studies have highlighted long-term, disease-specific complications, such as human papilloma virus susceptibility in IL-2Rγ (X-linked SCID due to IL-2Rγ deficiency), JAK3, and IL-7R deficiencies,[6,10,11] alkylator-related complications in *DCLRE1C* deficiency,[12] and extrahematopoietic manifestations in adenosine deaminase deficiency.[13] Furthermore, the quality of early immune reconstitution (which is predictive of long-term immune reconstitution) and the quality of B-cell function were found to be important predictive factors of the long-term clinical outcome.[5,6,9] In this context, we observed the onset of persistent hepatitis in 11 patients with SCID followed

up after HSCTor GTat Necker-Children's Hospital (Paris, France). These patients are referred to hereafter as the SCIDH1 group. We used a number of techniques (including pathology assessments, virologic screens, and multiomics experiments) to characterize the pathophysiology of these patients' condition.

We found that all the patients in the SCIDH+ group displayed a combination of liver $CD8^+$ T-cell infiltration, a chronic enteric viral infection, and the expansion of strongly activated memory $CD8^+$ T cells bearing type I and II interferon signatures. Moreover, we found that the absence of B-cell function and transplantation without myeloablation were strongly associated risk factors for persistent hepatitis. This condition (which we have named "enteric virus infection associated with hepatitis" [EVAH]) was cured in 5 patients after partially myeloablative retransplantation or GT, leading to an immune reconstitution and viral clearance.

METHODS

Pathology assessments

Paraffin-embedded sections (3-μm thick) were prepared and stained by hematoxylin-eosin saffron or Gordon-Sweet reagent. Immunohistochemistry was performed on a Leica Bond III automate (Leica Microsystems, Wetzlar, Germany) with either BOND ER1 (pH 6) or BOND ER2 (pH 9) epitope retrieval solutions (Leica Microsystems), depending on the primary antibodies. BOND Polymer Refine Detection kits (Leica Microsystems) with diaminobenzidine were used for detection. The sections were probed with primary antibodies against CD3 (CD3 polyclonal, A0452501; Agilent, Santa-Clara, Calif), CD20 (L26, M075501; Agilent), CD4 (4B12, F/MS-1528-S1; MM Brignais, France), CD8 (C8/144B, M710301; Agilent), granzyme B (11F1, GRAN-B-L-CE; Leica Microsystems), and CK7 (Clone OV-TL 12/30, M701801; Agilent).

Detection of adenovirus and enterovirus

Total nucleic acids were extracted from 200 μL of lysis buffer with a Nuclisens Extraction Kit for EMAG (Biomérieux, Marcy l'Etoile, France) and eluted in 100 μL of RNase-free water. The nucleic acids were amplified with the Adenovirus R-GENE assay and the Enterovirus R-GENE assay (Biomérieux) on an AB7500 system (Applied Biosystems, Waltham, Mass).

Detection of human Aichi virus

Nucleic acids from stool samples were extracted after lysis in a Nuclisens lysis buffer (Biom erieux). Total nucleic acids were extracted from 200 μL of lysis buffer with a Nuclisens Extraction Kit for EMAG (Biomérieux) and eluted in 100 μL of RNase-free water. We used previously described "in-house" RT-PCR assays targeting the viral 59 untranslated transcribed region[14] and the VP0[15] (capsid protein region) on a LightCycler 480 (Roche Diagnostics, Meylan, France), with some technical adjustments. After reverse transcription at 50°C for 20 minutes and initial denaturation at 95°C for 20 seconds, the RNAs were amplified in 45 cycles with a standard TaqMan 2-step protocol (60°C for 30 seconds and

95°C for 60 seconds). As a quality check, positive controls from the French National Reference Center for Viral Gastroenteritis (Dijon, France) were included in all experiments.

Detection of norovirus, sapovirus, astrovirus, and rotavirus

We used a qualitative, multiplex, real-time PCR assay (QIAstat Gastrointestinal Panel, Qiagen, Hilden, Germany) to detect norovirus GI, norovirus GII, rotavirus, sapovirus, astrovirus, and adenovirus 40/41 in human stool samples. In accordance with the manufacturer's instructions, 200 μL of stool suspension in FecalSwab medium was loaded into the test cartridge.

Isolation of PBMCs and plasma collection

Peripheral blood samples were collected in lithium heparin tubes and centrifuged at 2300 rpm for 10 minutes to collect supernatant (plasma). PBMCs were isolated by Ficoll density gradient centrifugation (2200 rpm without break for 30 minutes; Eurobio Scientific, Les Ulis, France) and washed twice in PBS (Thermo Fisher Scientific, Illkirch, France) by centrifugation at 1500 rpm for 5 minutes. Lastly, the PBMC pellet was resuspended in FBS (Gibco, Thermo Fisher Scientific) with 10% dimethyl sulfoxide (Sigma-Aldrich, St Quentin Fallavier, France) and frozen.

Cytometry by time of flight

PBMCs from 4 patients in the SCIDH+ group and 7 patients in the SCIDH– group were analyzed using cytometry by time of flight (CyTOF) (Maxpar Direct Immune Profiling System, Fluidigm, Les Ulus, France) including a 30-marker antibody panel (Fluidigm; ref. no. 201325). PBMCs (3×10^6) resuspended in 300 μL of Maxpar Cell Staining Buffer were incubated for 10 minutes at room temperature after the addition of 5 μL of Human TruStain FcX (BioLegend Europe, Amsterdam, the Netherlands). Then, the buffer was directly added to the dry antibody cocktail containing 30 antibodies (to which we added 1 μL of anti-PD1 coupled to 165Ho and 1 μL of anti-Tim3 coupled to 169Tm from Fluidigm) for 30 minutes. All samples were washed 3 times in Maxpar Cell Staining Buffer and then fixed in 1.6% paraformaldehyde (Sigma-Aldrich) for 10 minutes. After centrifugation, the PBMCs were incubated overnight in Fix and Perm Buffer with 1:1000 of iridium inter-calator (pentamethylcyclopentadienyl-Ir (III)-dipyridophenazine, Fluidigm) and frozen at −80°C before measurements.

Preparation of the single-cell RNA library

We analyzed 5 patients from the SCIDH+ group (P1–P5), 7 patients from the SCIDH− group, and 2 controls (P2's mother/donor and P4's mother/donor) in 2 single-cell experiments. The single-cell RNA (scRNA) libraries were generated using the Chromium Single Cell 3′ Library & Gel Bead Kit v.3 (10x Genomics, Pleasanton, Calif) according to the manufacturer's protocol. Briefly, cells were counted and diluted to 1,000 cells/μL in PBS + 0.04% BSA and 20,000 cells were loaded into the 10x Genomics Chromium Controller to generate an emulsion of singe-cell beads. After reverse transcription, the gel beads were lysed. Barcoded cDNA was isolated and amplified in PCRs. Following fragmentation, end repair, and A-tailing, sample indexes were added during index PCRs. The purified libraries

were sequenced on a No-vaseq (Illumina, Evry-Courcouronnes, France) with 28 Read 1 cycles, 8 Index 1 cycles (i7), and 91 Read 2 cycles.

Statistical analysis of the cohort as a whole

The characteristics of the patients and the HSCT procedures (molecular diagnosis, age at transplant, sex, conditioning regimen [CR], the quality of T-cell immune reconstitution 1 year after HSCT, and the quality of B-cell function after HSCT [defined as a continued requirement for immunoglobulin replacement therapy (IgRT)]) were included as potential predictors. The molecular diagnoses were grouped as follows: IL-2Rγ, JAK3, and IL-7R deficiencies in group 1; RAG1, RAG2, and DCLRE1C deficiencies in group 2; and other deficiencies in group 3. CRs were grouped as myeloablative conditioning versus no conditioning or reduced-intensity conditioning. The quality of T-cell immune reconstitution at 1-year posttransplant was defined as good when the $CD4^+$ T-cell count was more than 750/μL and/or the naive $CD4^+$ T-cell count was more than 500/μL; these thresholds were recently shown to be predictive of a good clinical outcome.[5] The characteristics of the SCIDH+ versus SCIDH− groups were compared in a chi-square test.

A decision tree that distinguished between the SCIDH+ and SCIDH− groups was built in a classification and regression tree analysis with the following variables: molecular diagnosis, CR, quality of T-cell immune reconstitution 1 year after HSCT, and persistence of IgRT after HSCT. The classification and regression tree analysis selects the most predictive variable after the data are split into 2 child nodes; the process is repeated further until splits no longer improve the purity of the terminal nodes.

RESULTS

Occurrence of chronic hepatitis after HSCT or GT

P1 to P11 were identified by the occurrence of persistent hepatitis during their follow-up. The patients had undergone HSCT or GT (with or without nonmyeloablative CR) for SCID in their first years of life (from 1983 to 2013) without or after a nonmyeloablative CR. All but 1 of the HSCT donors were haploidentical; P5 was the recipient of a matched sibling transplant.[16,17] Ten patients suffered from X-linked SCID due to IL-2Rγ deficiency, and 1 patient suffered from Artemis (DCLRE1C) deficiency. In all transplanted recipients, we observed a split chimerism with donor T cells and (mainly) recipient myeloid cells and B cells. NK-cell lymphopenia was noted in all patients (Table I). All patients failed to achieve satisfactory B-cell function and were still on IgRT. Early T-cell development and thymic output (as evaluated by the absolute $CD4^+$ T-cell and naive $CD4^+$ T-cell counts at 1 and 2 years after transplantation) were satisfactory (total $CD4^+ > 750$ cells/μL and naive $CD4^+ > 500$ cells/μL) in 6 patients (P1, P4, P5, P6, P8, and P9) and poor in 5 patients (P2, P3, P7, P10, and P11) (Fig 1).[5]

Elevated liver enzymes were detected at a median age of 6 years (range, 3–25 years) and persisted for a median follow-up of 4 years (range, 1.5–19 years) after onset. The transient appearance of psoriasiform skin lesions was noted for 3 patients (P1, P4, and P8). Splenomegaly and mild thrombocytopenia were also noted for 3 patients (P1, P6, and P7).

Nephromegaly was recorded in P7. All but 2 patients (P8 and P9) displayed a slowing in their height and weight gains (Fig 1; see also Fig E1 in this article's Online Repository at www.jacionline.org). Intermittent diarrhea and abdominal bloating were observed in 5 patients (P1, P5, P7, P10, and P11). Various immunosuppressive treatments (including corticosteroids, sirolimus, CTLA-4 agonist, anti-TNF agents, and Janus kinase inhibitors) and an antiviral drug (ganciclovir) were ineffective (Table I). In P5, the signs and symptoms of hepatitis and digestive tract disorders disappeared spontaneously 2 years after onset.

Significant changes in the immune phenotype were observed concomitantly with the hepatitis (Fig 1; see also Fig E1): a fall in both naive $CD4^+$ and $CD8^+$ T-cell counts and an expansion of effector memory (EM) $CD8^+$ T cells and/or EM T cells reex-pressing CD45RA (Fig 1). It is noteworthy that P5's naive T-cell count increased following the resolution of hepatitis. TCRVβ CDR3 spectratyping of the peripheral blood T-cell repertoire (in P1–P6) revealed a low level of diversity in all patients, with distinct TCR Vβ CDR3 sequences in the expanded clones (see Fig E2 in this article's Online Repository at www.jacionline.org).

Liver pathology showed $CD8^+$ T-cell infiltration

We analyzed a total of 27 liver biopsies from the 11 patients in the SCIDH1 group (see Table E1 in this article's Online Repository at www.jacionline.org). All the samples had very similar features and were characterized by centrilobular mononuclear infiltrates of variable intensity (mimicking granulomatous formations in 6 cases) mostly composed of $CD8^+$ T cells. Granzyme B staining was partially positive on $CD8^+$ T cells (see Fig E3, A–C, in this article's Online Repository at www.jacionline.org). The liver architecture was preserved initially, but 6 patients developed nodular formations reminiscent of nodular regenerative hyperplasia (NRH). Minimal fibrosis also very slowly progressed. The bile duct architecture was preserved in 5 cases; a mild, progressive, ductular reaction was noted in 5 patients; and concentric periductal fibrosis compatible with sclerosing cholangitis was observed in P3 (Fig E3). Digestive tract biopsies were performed in 6 patients. Partial villous atrophy was noticed on duodenal biopsies of P1, P2, and P10. Mild colitis was found in P5 and P7. Spleen and lymph node biopsies were also performed in P6 and showed a massive infiltration of $CD8^+$ T cells (Fig E3, D). Of note, findings for serum autoantibodies associated with autoimmune hepatitis were negative.

Detection of enteric viruses using metagenomic next-generation sequencing in patients from the SCIDH+ group

PCR-based screens for hepatotropic viruses in the plasma (hepatitis A, B, C, E, and enterovirus) and whole-blood samples (EBV, cytomegalovirus, and adenovirus) of the patients in the SCIDH+ group were negative. The available frozen liver biopsies (n = 13), a spleen biopsy (P6), and a gut biopsy (P10) were analyzed retrospectively with metagenomic next-generation sequencing (Table I). Sequences of human Aichi virus 1 (genotype B) were identified in P1 and P7 (in the liver biopsy) and P6 (in both the spleen and lymph nodes) and were confirmed by targeted RT-PCR. Norovirus (genogroup GII) was identified in a liver biopsy of P2 7 years after onset of hepatitis and in a gut biopsy of P10. In 3 patients who had protracted diarrhea, either sapovirus (P1 and P5) or norovirus (P10) was repeatedly identified in stool samples by RT-PCR. Additional screening of stools identified

persistent shedding of norovirus despite the absence of digestive symptoms in P2, P3, and P4. Screening by multiplex PCR assay (norovirus, sapovirus, astrovirus, and rotavirus) and simplex PCR assay (enterovirus, adenovirus, and human Aichi virus) was performed in stool samples from 13 consecutive patients with SCID (IL-2Rγ or JAK3 deficiency) who had undergone HSCT. The patients had undergone HSCT between 7 and 37 years previously, using a very similar approach: the absence of myeloablation in most cases and a mismatched related donor that led to continuation of IgRT in the long-term after transplantation. The patients' liver enzyme levels were normal, and a screen for enteric viruses was negative. Henceforth, this group of patients will be referred to as the SCIDH− group (see Table E2 in this article's Online Repository at www.jacionline.org).

A multiomics analysis highlighted an activated CD8$^+$ T-cell phenotype and strong type I and II IFN signatures in PBMCs

Mass cytometry (CyTOF) and scRNA sequencing (scRNAseq) were performed on PBMCs from 5 patients in the SCIDH+ group (P2–P6 for CyTOF and P1–P5 for scRNAseq), 7 patients in the SCIDH− group, and 2 healthy controls (P2's and P4's donors, for scRNAseq only). The patients' treatments at the time of PBMCs sampling are presented in Table I.

The CyTOF and scRNAseq analysis confirmed the blood immunophenotyping results with a drop in the proportion of naive CD4$^+$ and CD8$^+$ T cells and an increase in the proportion of total CD8$^+$ T cells (mainly composed of EM and EM T cells re-expressing CD45RA in the SCIDH1 group) (Fig 2, A; see also Figs E4, B, and E5, A–D, in this article's Online Repository at www.jacionline.org). Furthermore, CyTOF enabled us to identify a particular cluster of EM CD8$^+$ T cells. The cluster was CD38^{high}, HLA-DR^{high} (both known markers of activated CD8^1 T cells), and CD127 (IL-7R)^{low} (a known marker of chronic viral infection)[18,19] and was significantly enriched in T cells from patients in the SCIDH+ group (Fig 2, B and C; see also Figs E4, A and B, and E6, B and C, in this article's Online Repository at www.jacionline.org). Because principal-component analysis of the scRNAseq data revealed clustering in the SCIDH+ group with regard to CD8$^+$ T cells and, to a lesser extent, dendritic cells (DCs) and monocytes, we focused the analysis on CD8$^+$ T cells (Fig 3, A; see also Fig E6, A). Positively differentially expressed genes in CD8$^+$ T cells from the SCIDH+ group compared with those from the SCIDH− group or controls mainly belonged to IFN-stimulated genes (ISGs) such as *IFIT1*, *IFIT3*, *OASL*, *IFI27*, *IFI44L*, or *IFI44* (Fig 3, B; see also this article's Online Repository at www.jacionline.org). This IFN environment was further shown by pathway enrichment analysis (Fig 3, C) and type I or II IFN signatures (Fig 3, D and E). Of note, CD8$^+$ T cells from the SCIDH+ group did not exhibit enrichment in genes associated with exhaustion except for LAG3 (Fig 3, F). In contrast, CD4$^+$ T cells from patients in the SCIDH+ group displayed higher expression of PD1 and CD57 (as shown by CyTOF; Fig E6, D) and of exhaustion-associated genes (as shown by scRNAseq; Fig E6, E). Genes associated with cytotoxicity or apoptosis were not differentially expressed (Fig E6, F). Subclustering of the CD8$^+$ T cells from the scRNAseq experiment identified 10 clusters (Fig 4, A; see also Figs E5, E, and E6, F). Of these, cluster 6 was most strongly represented in the SCIDH+ group (Fig 3, B); given that most of the cluster's marker genes were ISGs, we refer to the T cells as ISG^{high} CD8$^+$ (Fig 3, C–F).

Taken together, these results show that the SCIDH+ group had an expansion of highly activated $CD8^+$ T cells with enhanced response to type I and II IFNs concomitantly with protracted enteric viral infection. Of note, this high level of response to IFNs was also found in other immune subsets such as classical dendritic cells (cDCs), plasmacytoid dendritic cells (pDCs), and monocytes (Fig 3, E and F) and was confirmed by RT-qPCR of 6 ISGs on whole-blood samples (see Fig E7, A, in this article's Online Repository at www.jacionline.org). In addition, RNA-Scope for CXCL9 and IFN-γ was performed on liver biopsies of P1, P2, and P3 and spleen biopsy of P6, showing an enrichment in IFN-γ–positive cells (Fig E3, E). Cytokine levels were measured by Legendplex (San Diego, Calif) or SIMOA (Billerica, Mass) in sera of 5 patients (P2–P6) and showed a trend for increased inflammatory cytokines with interindividual variabilities (Fig E7, B and C).

Overall risk factors for hepatitis in patients with SCID recipient of cellular therapy (HSCT or GT)

Of the 155 patients with SCID who were alive 2 years after their HSCT (n = 141 since 1972) or GT (n = 14 since 1999) at Necker-Children's Hospital, 114 had been regularly monitored for liver enzyme levels (Fig 5; see also Table E3 in this article's Online Repository at www.jacionline.org). Overall, 11 (9.6%) of the 141 patients displayed hepatitis associated with $CD8^+$ T-cell expansion and (in 8 of the 11) the persistent presence of enteric viruses. The SCIDH+ and SCIDH− groups did not differ significantly with regard to the sex ratio, maintenance of IgRT, or CR intensity (Table E3). The cumulative risk of developing hepatitis at the age of 15 years was 25% for patients with no conditioning or low-intensity conditioning (oral busulfan 8 mg/kg and cyclophosphamide 200 mg/kg) and who were on IgRT versus 0% ($P = .00018$) for patients in the other groups (Fig 5, B).

Outcome and curative treatments of hepatitis

Three of the 11 patients in the SCIDH+ group died: P7 died of progressive protein-losing enteropathy and portal hypertension, P10 died of protein-losing enteropathy, and P11 died of acute graft-versus-host disease after the administration of a hematopoietic stem cell boost had been prompted by the patient's poor general condition. In view of his worsening condition, P1 underwent a lentiviral GT at the US National Institute of Health (Bethesda, Md; ClinicalTrials.gov identifier: NCT01306019) at the age of 13 years (ie, 7 years after the onset of hepatitis).[20] GT was preceded by conditioning (upfront alemtuzumab 1 mg/kg total dose; D-21 to D-20 and busulfan 6 mg/kg total dose, with a targeted area under the curve of 18–20 mg $ h/L). Interestingly, reductions in diarrhea and liver enzyme levels were noted immediately on treatment with the anti-CD52 alemtuzumab. The clinical and immunologic outcomes were remarkable. The stools and abdominal bloating normalized within 3 months. Sapovirus in the stool samples was no longer detectable 3 months after GT. P1's general health status improved quickly, and he started to gain height and weight more rapidly (Fig 1). The patient's liver enzyme levels normalized 9 months after GT, concomitantly with the disappearance of circulating initial donor $CD8^+$ T cells. Autologous T-, B-, and NK-cell counts and naive $CD4^+$ and $CD8^+$ T-cell counts increased progressively during the first year. IgRTwas discontinued 2 years after GT because satisfactory vaccine responses were observed. P2 and P3 were subsequently included in the same protocol and underwent GT. The GT procedures were uneventful.

The liver enzyme level fell in both patients, and stool samples were free of norovirus 6 months after GT. P4 underwent HSCT with a matched, unrelated donor at the age of 7 years (18 months after the onset of hepatitis). He was conditioned with alemtuzumab, busulfan (area under the curve, 56 mg $ h/L), and fludarabine, which resulted in full donor chimerism (see this article's Online Repository). P4's clinical and immunologic outcomes were excellent 2 years after HSCT, the liver enzyme levels normalized rapidly, and norovirus was no longer detected in stool samples 18 months after HSCT. Cessation of IgRT is planned. P6 underwent HSCT with a matched sibling donor (his brother). Despite full engraftment, P6 developed several complications (including graft-vs-host disease, post-HSCT EBV-related lymphoproliferation, and a disseminated mycobacterial infection) that delayed his immune reconstitution and recovery. At the age of 25 years, P7 underwent a second HSCT with a matched sibling donor (his brother). He achieved full donor chimerism and experienced good clinical and biochemical outcomes including the disappearance of hepatitis (see this article's Online Repository). IgRT was discontinued 2 years after HSCT. P5 recovered spontaneously from the hepatitis concomitantly with the clearance of sapovirus and improvement of T-cell subset repartition (Fig 1).

DISCUSSION

Our long-term follow-up of patients with SCID having undergone HSCT or GT identified 11 cases of EVAH: late-onset slowly progressing, chronic hepatitis with the infiltration of $CD8^+$ T cells, progressive failure to thrive, expansion of EM $CD8^+$ T cells, and (in 2 cases) chronic lymphoproliferation and splenomegaly. Enteric viruses were detected in liver biopsies and/or stool samples in all 8 patients who could be screened. Poor B-cell reconstitution (ie, a continued requirement for IgRT) and the absence of myeloablation before HSCT were the main risk factors for this chronic hepatitis. Although the condition was severe and led to death in 3 cases, it could be cured by GT or second HSCT after myeloablation.

A multiomics analysis of PBMCs enabled us to identify and characterize activated EM $CD8^+$ T cells with a strong type I or II IFN signature. This phenomenon was further exemplified by the identification of a prominent ISG^{high} $CD8^+$ T-cell cluster in the SCIDH+ group. It is noteworthy that monocytes and DCs might have contributed to the inflammatory process because the cell types also displayed an IFN^{high} signature. Remarkably, the $CD8^+$ T cells did not have an obvious exhausted phenotype after several years of viral persistence as shown by analysis of pathway enrichment, gene expression (scRNAseq), and PD1 expression (CyTOF).

In P6 (who received GT early in life), splenomegaly and the expansion of circulating $CD8^+$ T cells led to suspect lymphoma, but the latter was ruled out by molecular analyses. For the other patients, we initially thought that these $CD8^+$ T cells were causing an autoinflammatory or autoimmune condition in the context of a persistent partial immunodeficiency, which was notably characterized by a drop in the naive T-cell count. However, autoantibodies were not detected and the condition did not resolve on treatment with immunosuppressants. Importantly, enteric viruses were repeatedly detected in these patients but were absent in the SCIDH− group. One can therefore reasonably hypothesize that (1) the persistent hepatitis in the SCIDH+ group was due to an enteric human Aichi

virus A/sapovirus/norovirus infection that could not be controlled by the patient's immune system and (2) this infection led to chronic gut inflammation and leakage of the gut barrier. As has been observed in a mouse model of chronic cytomegalovirus infection, virus-induced type I IFN production might have accentuated the increase in gut permeability.[21] There is no formal proof of a causal relationship with an enteric virus infection because we were unable to show that the expanded $CD8^+$ T cells specifically recognized viral epitopes. However, the SCIDH+ phenotype is reminiscent of that observed in patients with X-linked agammaglobulinemia (XLA) and a chronic enteric virus infection[22] and in immunocompetent patients with concomitant hepatitis and influenza.[23] It is noteworthy that 2 patients with XLA and 2 with acquired hypogammaglobulinemia after rituximab were reported to have chronic Aichi virus infection,[24–26] and that chronic hepatitis and NRH are underrecognized but relatively common features of XLA.[27] Chronic norovirus infection is also seen in various forms of immunodeficiency, including common variable immunodeficiency and XLA.[28] Lastly, transient hepatitis is a common feature of acute norovirus infections in immunocompetent patients.[29,30]

All the patients in the SCIDH+ group required IgRT because of a persistent deficiency in antibody production by host B lymphocytes. Hence, EVAH might be triggered primarily by defective antibody-mediated neutralization of enteric viruses at the gut barrier, leading to chronic infection and a $CD8^+$ T-cell/monocyte-driven immunopathology. Moreover, we cannot exclude a viral-induced inhibition of B-cell capacity to present antigens that could facilitate the chronic infection as it was described quite recently for norovirus.[31,32] Nevertheless, the importance of $CD8^+$ T cells in this immunopathologic process was emphasized by our observation of liver enzyme normalization after GT or a second HSCT. An improvement was even observed during the CR despite the persistence of viral shedding. Studies in the mouse have demonstrated the importance of humoral responses for clearing norovirus infections and the lack of redundancy between type I/II IFN responses and T-cell responses.[33,34] We also cannot rule out a possible role of NK-cell and/or innate lymphoid cell deficiencies—a hallmark of patients having undergone nonmyeloablative HSCT and who display split chimerism with T cells as the only donor-derived cells.[35] One could suppose that incomplete correction of the T-cell immunodeficiency contributes to EVAH as suggested by the drop in the naive T-cell count. In fact, the initial T-cell reconstitution was good in most patients, and the usual features of T-cell immunodeficiency (eg, susceptibility to certain infections) were lacking. Furthermore, the early quality of T-cell immune reconstitution did not appear to be a risk factor in univariate and multivariate analyses. Furthermore, the observed drop in the naive T-cell count might have been a consequence of the chronic infection, because it is also observed in patients with XLA with a chronic enteric virus infection.[24] Plus, enteric viruses might escape neutralization by the IgG provided by IgRT because of an inefficient neutralization titer and/or inadequate recognition of epitopes on highly mutated viruses in the context of chronic shedding.[36]

We observed that EVAH was cured by myeloablative HSCT or GT, indicating that the viral infection can be controlled by effective immune effector cells, including B cells. Importantly, the outcomes of repeat cell therapy in the patients in the SCIDH+ group suggest that EVAH (including NRH) is reversible. Hence, given the progressive course of EVAH (regardless of symptomatic treatments), it makes sense to offer potentially

curative treatment to these patients. Careful, long-term post-HSCTor post-GT monitoring of patients with SCID is recommended, including broad screens for enteric viruses in subjects with posttransplantation B-cell dysfunction and the early detection of immunopathologic processes. It remains to be determined whether preemptive GT or repeat HSCT (ie, before the likely onset of EVAH) would be of value in patients without B-cell reconstitution if an HLA-identical donor is available. Our present results also emphasize the importance of including some degree of myeloablation in the CR for HSCT or GT in an indication of SCID to ensure effective B-cell function thereafter.

We sincerely thank the patients and their families for their trust. We are also grateful to the clinical staff in the Pediatric Immuno-Hematology and Rheumatology Unit at Necker-Children's Hospital. We thank all the staff from the genomics, bioinformatics, cytometry, and single-cell core facilities at the Imagine Institute. Lastly, we thank the staff at the CyPS Salpêtri ere cytometry facility for technical assistance and helpful advice.

Supplementary Material

Refer to Web version on PubMed Central for supplementary material.

Authors

Quentin Riller, MD, MSc[a,b,*], Jacques Fourgeaud, MD, PhD[a,c,d,e,*], Julie Bruneau, MD, PhD[a,f,g,*], Suk See De Ravin, MD, PhD[h], Grace Smith, MD, PhD[i], Mathieu Fusaro, MD, MSc[j], Samy Meriem, PharmD[k], Aude Magerus, PhD[a,b], Marine Luka, MSc[l], Ghaith Abdessalem, PhD[l], Ludovic Lhermitte, MD, PhD[a,m,n], Anne Jamet, MD, PhD[a,c,n], Emmanuelle Six, PhD[a,o], Alessandra Magnani, MD, PhD[p], Martin Castelle, MD[q], Romain Lévy, MD, PhD[a,q,r], Mathilde M. Lecuit, MD, MSc[q], Benjamin Fournier, MD, PhD[a,q], Sarah Winter, MD, PhD[a,q], Michaela Semeraro, MD, PhD[a,s], Graziella Pinto, MD[t], Hanène Abid, MD[a,c], Nizar Mahlaoui, MD, PhD[q], Nathalie Cheikh, MD[u], Benoit Florkin, MD[v], Pierre Frange, MD, PhD[a,c,q], Eric Jeziorski, MD[w], Felipe Suarez, MD, PhD[a,g,x], Françoise Sarrot-Reynauld, MD[y], Dalila Nouar, MD[z], Dominique Debray, MD, PhD[aa], Florence Lacaille, MD[bb], Capucine Picard, MD, PhD[j,cc], Philippe Pérot, PhD[d,dd], Béatrice Regnault, PhD[d,dd], Nicolas Da Rocha, PhD[d,dd], Camille de Cevins, PhD[a,ee,ff], Laure Delage, PhD[a,b], Brieuc P. Pérot, PhD[a,ee], Angélique Vinit, MSc[gg], Francesco Carbone, PhD[a,l,ee], Camille Brunaud, MSc[a,b], Manon Marchais, MSc[a,b], Marie-Claude Stolzenberg, PhD[a,b], Vahid Asnafi, MD, PhD[a,m,n], Thierry Molina, MD, PhD[a,f], Frédéric Rieux-Laucat, PhD[a,b], Luigi D. Notarangelo, MD, PhD[h], Stefania Pittaluga, MD, PhD[hh], Jean Philippe Jais, PhD[a,k], Despina Moshous, MD, PhD[a,q,ii,‡], Stephane Blanche, MD[a,q,‡], Harry Malech, MD, PhD[h,‡], Marc Eloit, PhD[d,dd,jj,§], Marina Cavazzana, MD, PhD[a,m,o,§], Alain Fischer, MD, PhD[q,kk,§], Mickaël M. Ménager, PhD[a,l,e,e,§], Bénédicte Neven, MD, PhD[a,b,q,§]

Affiliations

[a]University of Paris Cité, Paris, France;

[b]Laboratory of Immunogenetics of Pediatric Autoimmune Diseases, Imagine Institute, INSERM UMR 1163, Paris, France;

[c]Microbiology Department, Necker-Children's Hospital, Assistance Publique-Hôpitaux de Paris, Paris, France;

[d]Pathogen Discovery Laboratory, Institut Pasteur, Université de Paris, Paris, France;

[e]Prise en Charge des Anomalies Congénitales et leur Traitement, Unit 7328, Imagine Institute, University of Paris Cité, Paris, France;

[f]Pathology Department, Necker-Children's Hospital, Assistance Publique-Hôpitaux de Paris, Paris, France;

[g]Imagine Institute, INSERM UMR 1163, Laboratory of Molecular Mechanisms of Hematologic Disorders and Therapeutic Implications, Necker-Children's Hospital, Assistance Publique-Hôpitaux de Paris, Paris;

[h]Laboratory of Clinical Immunology and Microbiology, National Institute of Allergy and Infectious Diseases, National Institutes of Health, Bethesda, Md;

[i]Center for Cancer Research, National Cancer Institute, National Institutes of Health, Bethesda;

[j]Study Center for Primary Immunodeficiencies, Necker-Children's Hospital, Assistance Publique-Hôpitaux de Paris, Paris, France;

[k]Laboratory of Biostatistics, University of Paris Cité, Paris, France;

[l]Labtech Single-Cell@Imagine, Imagine Institute, INSERM UMR 1163, Paris, France;

[m]Laboratory of Onco-Haematology, Necker-Children's Hospital, Assistance Publique-Hôpitaux de Paris, Paris, France;

[n]Institut Necker-Enfants Malades (INEM), INSERM UMR 1151, Necker-Children's Hospital, Assistance Publique-Hôpitaux de Paris, Paris, France;

[o]Laboratory of Human Lympho-Hematopoiesis, Imagine Institute, INSERM UMR 1163, Paris, France;

[p]Department of Biotherapy, Necker-Children's Hospital, Assistance Publique-Hôpitaux de Paris, Paris, France;

[q]Pediatric Hematology-Immunology and Rheumatology Unit, Necker-Children's Hospital, Assistance Publique-Hôpitaux de Paris, Paris, France;

[r]Laboratory of Human Genetics of Infectious Diseases, Necker Branch, INSERM, Necker-Children's Hospital, Assistance Publique-Hôpitaux de Paris, Paris, France;

[s]Clinical Investigation Center, Clinical Research Unit, Necker-Children's Hospital, Assistance Publique-Hôpitaux de Paris, Paris, France;

[t]Pediatric Endocrinology, Gynecology, Diabetology, Necker-Children's Hospital, Assistance Publique-Hôpitaux de Paris, Paris;

[u]Pediatric Hematology Oncology Unit, University Hospital of Besançon, Besançon, France;

[v]Immuno-Hémato-Rhumatologie Pédiatrique, Service de Pédiatrie, CHR Citadelle, Liege, Belgium;

[w]Department of Pediatrics, Infectious Diseases, and Immunology, University of Montpellier, CHU Montpellier, Montpellier, France;

[x]Hematology Department, Necker-Children's Hospital, Assistance Publique-Hôpitaux de Paris, Paris;

[y]Service de Médecine Interne, Centre Hospitalier Universitaire Grenoble Alpes, Grenoble, France;

[z]Service d'Immunologie Clinique et d'Allergologie, Centre Hospitalier Régional Universitaire, Tours, France;

[aa]Pediatric Liver Unit, National Reference Center for Rare Diseases, Biliary Atresia and Genetic Cholestasis, Inflammatory Biliary Diseases and Autoimmune Hepatitis, ERN Rare Liver, Necker-Children's Hospital, Assistance Publique-Hôpitaux de Paris, Paris, France;

[bb]Gastroenterology-Hepatology-Nutrition Unit, Necker-Children's Hospital, Assistance Publique-Hôpitaux de Paris, Paris, France;

[cc]Laboratory of Lymphocyte Activation and Susceptibility to EBV Infection, Imagine Institute, INSERMUMR1163, Paris, France;

[dd]OIE Collaborating Center for the Detection and Identification in Humans of Emerging Animal Pathogens, Institut Pasteur, Paris, France;

[ee]Laboratory of Inflammatory Responses and Transcriptomic Networks in Diseases, Atip-Avenir Team, Imagine Institute, INSERM UMR 1163, Paris;

[ff]Artificial Intelligence & Deep Analytics (AIDA) Group, Data & Data Science (DDS), Sanofi R&D, Chilly-Mazarin, France;

[gg]Sorbonne Université, UMS037, PASS, Plateforme de Cytométrie de la Pitié-Salpêtrière CyPS, Paris;

[hh]National Cancer Institute, National Institutes of Health, Bethesda;

[ii]Laboratory of Genome Dynamics in the Immune System, Equipe Labellisée Ligue contre le Cancer, Imagine Institute, INSERM UMR 1163, Paris;

[jj]Ecole Nationale Vétérinaire d'Alfort, Maisons-Alfort, France;

[kk]Collège de France, Paris.

Acknowledgments

Q.R. is a recipient of an Institut Imagine MD-PhD fellowship (funded by the Fondation Bettencourt Schueller, France) and a Société Nationale Française de Médecine Interne fellowship. The work was funded by 2 grants from the Centre de Référence et d'Etude des Déficits Immunitaire (CEREDIH).

Abbreviations used

CR	Conditioning regimen
CyTOF	Cytometry by time of flight
DC	Dendritic cell
EM	Effector memory
EVAH	Enteric virus infection associated with hepatitis
GT	Gene therapy
HSCT	Hematopoietic stem cell transplantation
IgRT	Immunoglobulin replacement therapy
ISG	IFN-stimulated gene
mNGS	Metagenomic next-generation sequencing
NGS	Next-generation sequencing
NK	Natural killer
NRH	Nodular regenerative hyperplasia
SCID	Severe combined immunodeficiency
SCID-X1	X-linked SCID due to IL-2Rγ deficiency
scRNA	Single-cell RNA
scRNAseq	scRNA sequencing
XLA	X-linked agammaglobulinemia

REFERENCES

1. Gennery AR, Slatter MA, Grandin L, Taupin P, Cant AJ, Veys P, et al. Transplantation of hematopoietic stem cells and long-term survival for primary immunodeficiencies in Europe: entering a new century, do we do better? J Allergy Clin Immunol 2010;126:602–10.e1–11. [PubMed: 20673987]
2. Heimall J, Logan BR, Cowan MJ, Notarangelo LD, Griffith LM, Puck JM, et al. Immune reconstitution and survival of 100 SCID patients post-hematopoietic cell transplant: a PIDTC natural history study. Blood 2017;130:2718–27. [PubMed: 29021228]
3. Fischer A, Hacein-Bey-Abina S. Gene therapy for severe combined immunodeficiencies and beyond. J Exp Med 2020;217:e20190607. [PubMed: 31826240]
4. Cavazzana M, Bushman FD, Miccio A, Andr e-Schmutz I, Six E. Gene therapy targeting haematopoietic stem cells for inherited diseases: progress and challenges. Nat Rev Drug Discov 2019;18:447–62. [PubMed: 30858502]
5. Lankester AC, Neven B, Mahlaoui N, von Asmuth EGJ, Courteille V, Alligon M, et al. Hematopoietic cell transplantation in severe combined immunodeficiency: the SCETIDE 2006–2014 European cohort. J Allergy Clin Immunol 2022;149: 1744–54.e8. [PubMed: 34718043]

6. Neven B, Leroy S, Decaluwe H, Le Deist F, Picard C, Moshous D, et al. Long-term outcome after hematopoietic stem cell transplantation of a single-center cohort of 90 patients with severe combined immunodeficiency. Blood 2009;113:4114–24. [PubMed: 19168787]
7. Gatti RA, Meuwissen HJ, Allen HD, Hong R, Good RA. Immunological reconstitution of sex-linked lymphopenic immunological deficiency. Lancet 1968;292:1366–9.
8. Pai SY, Logan BR, Griffith LM, Buckley RH, Parrott RE, Dvorak CC, et al. Transplantation outcomes for severe combined immunodeficiency, 2000–2009. N Engl J Med 2014;371:434–46. [PubMed: 25075835]
9. Haddad E, Logan BR, Griffith LM, Buckley RH, Parrott RE, Prockop SE, et al. SCID genotype and 6-month posttransplant CD4 count predict survival and immune recovery. Blood 2018;132:1737–49. [PubMed: 30154114]
10. Laffort C, Le Deist F, Favre M, Caillat-Zucman S, Radford-Weiss I, Debré M, et al. Severe cutaneous papillomavirus disease after haemopoietic stem-cell transplantation in patients with severe combined immune deficiency caused by common gam-mac cytokine receptor subunit or JAK-3 deficiency. Lancet 2004;363:2051–4. [PubMed: 15207958]
11. Abd Hamid IJ, Slatter MA, McKendrick F, Pearce MS, Gennery AR. Long-term outcome of hematopoietic stem cell transplantation for IL-2RG/JAK3 SCID: a cohort report. Blood 2017;129:2198–201. [PubMed: 28209722]
12. Schuetz C, Neven B, Dvorak CC, Leroy S, Ege MJ, Pannicke U, et al. SCID patients with ARTEMIS vs RAG deficiencies following HCT: increased risk of late toxicity in ARTEMIS-deficient SCID. Blood 2014;123:281–9. [PubMed: 24144642]
13. Hassan A, Booth C, Brightwell A, Allwood Z, Veys P, Rao K, et al. Outcome of hematopoietic stem cell transplantation for adenosine deaminase-deficient severe combined immunodeficiency. Blood 2012;120:3615–24, quiz 3626. [PubMed: 22791287]
14. Nielsen ACY, Gyhrs ML, Nielsen LP, Pedersen C, Böttiger B. Gastroenteritis and the novel picornaviruses aichi virus, cosavirus, saffold virus, and salivirus in young children. J Clin Virol 2013;57:239–42. [PubMed: 23602437]
15. Kitajima M, Hata A, Yamashita T, Haramoto E, Minagawa H, Katayama H. Development of a reverse transcription-quantitative PCR system for detection and gen-otyping of aichi viruses in clinical and environmental samples. Appl Environ Microbiol 2013;79:3952–8. [PubMed: 23603673]
16. Touzot F, Dal-Cortivo L, Verkarre V, Lim A, Crucis-Armengaud A, Moshous D, et al. Massive expansion of maternal T cells in response to EBV infection in a patient with SCID-Xl. Blood 2012;120:1957–9. [PubMed: 22936741]
17. Hacein-Bey-Abina S, Hauer J, Lim A, Picard C, Wang GP, Berry CC, et al. Efficacy of gene therapy for X-linked severe combined immunodeficiency. N Engl J Med 2010;363:355–64. [PubMed: 20660403]
18. Carrette F, Surh CD. IL-7 signaling and CD127 receptor regulation in the control of T cell homeostasis. Semin Immunol 2012;24:209–17. [PubMed: 22551764]
19. Zhang SY, Zhang Z, Fu JL, Kang FB, Xu XS, Nie WM, et al. Progressive CD127 down-regulation correlates with increased apoptosis of CD8 T cells during chronic HIV-1 infection. Eur J Immunol 2009;39:1425–34. [PubMed: 19350559]
20. De Ravin SS, Wu X, Moir S, Anaya-O'Brien S, Kwatemaa N, Littel P, et al. Lentiviral hematopoietic stem cell gene therapy for X-linked severe combined immunodeficiency. Sci Transl Med 2016;8:335ra57.
21. Labarta-Bajo L, Nilsen SP, Humphrey G, Schwartz T, Sanders K, Swafford A, et al. Type I IFNs and CD8 T cells increase intestinal barrier permeability after chronic viral infection. J Exp Med 2020;217:e20192276. [PubMed: 32880630]
22. Bearden D, Collett M, Quan PL, Costa-Carvalho BT, Sullivan KE. Enteroviruses in X-linked agammaglobulinemia: update on epidemiology and therapy. J Allergy Clin Immunol Pract 2016;4:1059–65. [PubMed: 26883540]
23. Polakos NK, Cornejo JC, Murray DA, Wright KO, Treanor JJ, Crispe IN, et al. Kupffer cell-dependent hepatitis occurs during influenza infection. Am J Pathol 2006;168:1169–78. [PubMed: 16565492]

24. Bucciol G, Moens L, Payne K, Wollants E, Mekahli D, Levtchenko E, et al. Chronic Aichi virus infection in a patient with X-linked agammaglobulinemia. J Clin Immunol 2018;38:748–52. [PubMed: 30311057]
25. Meyts I, Bucciol G, Jansen K, Wollants E, Breuer J. Aichivirus: an emerging pathogen in patients with primary and secondary B-cell deficiency [published online ahead of print November 30, 2022]. J Clin Immunol. 10.1007/s10875-022-01410-6.
26. Bekassy Z, Ehinger M, Pronk LN, Pronk CJ, Bekassy Z, Ehinger M, et al. Immunologic control of disseminated Aichi virus infection in X-linked agammaglobulinemia by transplantation of TCR αβ-depleted haploidentical hematopoietic cells. J Clin Immunol 2022;42:1401–4. [PubMed: 35788939]
27. Nunes-Santos CJ, Koh C, Rai A, Sacco K, Marciano BE, Kleiner DE, et al. Nodular regenerative hyperplasia in X-linked agammaglobulinemia: an underesti-mated and severe complication. J Allergy Clin Immunol 2022;149:400–9.e3. [PubMed: 34087243]
28. Frange P, Touzot F, Debré M, Héritier S, Leruez-Ville M, Cros G, et al. Prevalence and clinical impact of norovirus fecal shedding in children with inherited immune deficiencies. J Infect Dis 2012;206:1269–74. [PubMed: 22872736]
29. Nakajima H, Watanabe T, Miyazaki T, Takeuchi M, Honda Y, Shimada N, et al. Acute liver dysfunction in the course of norovirus gastroenteritis. Case Rep Gastroenterol 2012;6:69–73. [PubMed: 22423242]
30. Khayat AA, Telega GW. Persistent elevation of aminotransferases in liver transplant in association with chronic norovirus infection. Clin Mol Hepatol 2019;25: 408–11. [PubMed: 31062535]
31. Zhu S, Jones MK, Hickman D, Han S, Reeves W, Karst SM. Norovirus antagonism of B cell antigen presentation results in impaired control of acute infection. Mucosal Immunol 2016;9:1559–70. [PubMed: 27007673]
32. Upasani V, Rodenhuis-Zybert I, Cantaert T. Antibody-independent functions of B cells during viral infections. PLoS Pathog 2021;17:e1009708. [PubMed: 34293057]
33. Karst SM, Wobus CE, Lay M, Davidson J, Virgin HW. STAT1-dependent innate immunity to a Norwalk-like virus. Science 2003;299:1575–8. [PubMed: 12624267]
34. Chachu KA, Strong DW, LoBue AD, Wobus CE, Baric RS, Virgin HW. Antibody is critical for the clearance of murine norovirus infection. J Virol 2008;82: 6610–7. [PubMed: 18417579]
35. Vély F, Barlogis V, Vallentin B, Neven B, Piperoglou C, Ebbo M, et al. Evidence of innate lymphoid cell redundancy in humans. Nat Immunol 2016;17:1291–9. [PubMed: 27618553]
36. Afridi SQ, Usman Z, Donakonda S, Wettengel JM, Velkov S, Beck R, et al. Prolonged norovirus infections correlate to quasispecies evolution resulting in struc-tural changes of surface-exposed epitopes. iScience 2021;24:102802. [PubMed: 34355146]

Key messages

- Hepatitis is frequently late after HSCT or GT in SCID and is related to an inappropriate immune response to chronic enteric viral infection.
- Absence of B-cell function and absence of myeloablation are risk factors for this condition. Second procedure with myeloablation is curative.

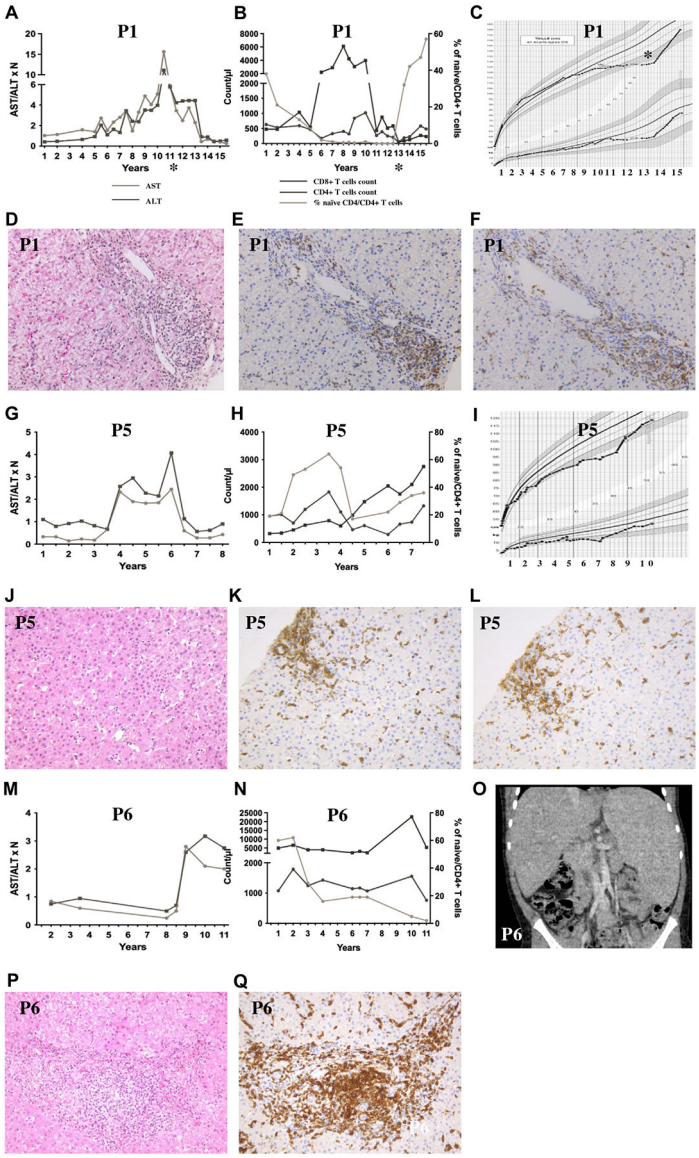

FIG 1.

Late-onset hepatitis, failure to thrive, and concomitant immunophenotypic changes. Changes over time in laboratory and clinical variables for P1 (**A-C**), P5 (**G-I**), and P6 (**M-O**). *A, G*, and *M*, Serum transaminase levels (AST for aspartate aminotransferase in orange and ALT for alanine aminotransferase in blue) over time expressed as a multiple of the normal value. *B, H*, and *N*, Changes over time in $CD4^+$ T-cell counts (*dark green*), $CD8^+$ T-cell counts (*purple*), and percentage of naive $CD4^+$ T cells among $CD4^+$ T cells (*light green*). *C* and *I*, Weight (lower curve) and height (upper curve) changes over time. *O, CT* scan of the abdomen (axial view) of P6, 9 months after the onset of hepatitis. Histological assessments of liver biopsies from P1 (**D-F**), P5 (**J-L**), and P6 (**P** and **Q**). *D, J*, and *P*, Hematoxylin-eosin-saffron staining ×200. *E, K*, and *Q*, CD3 staining. *F* and *L*, CD8 staining.

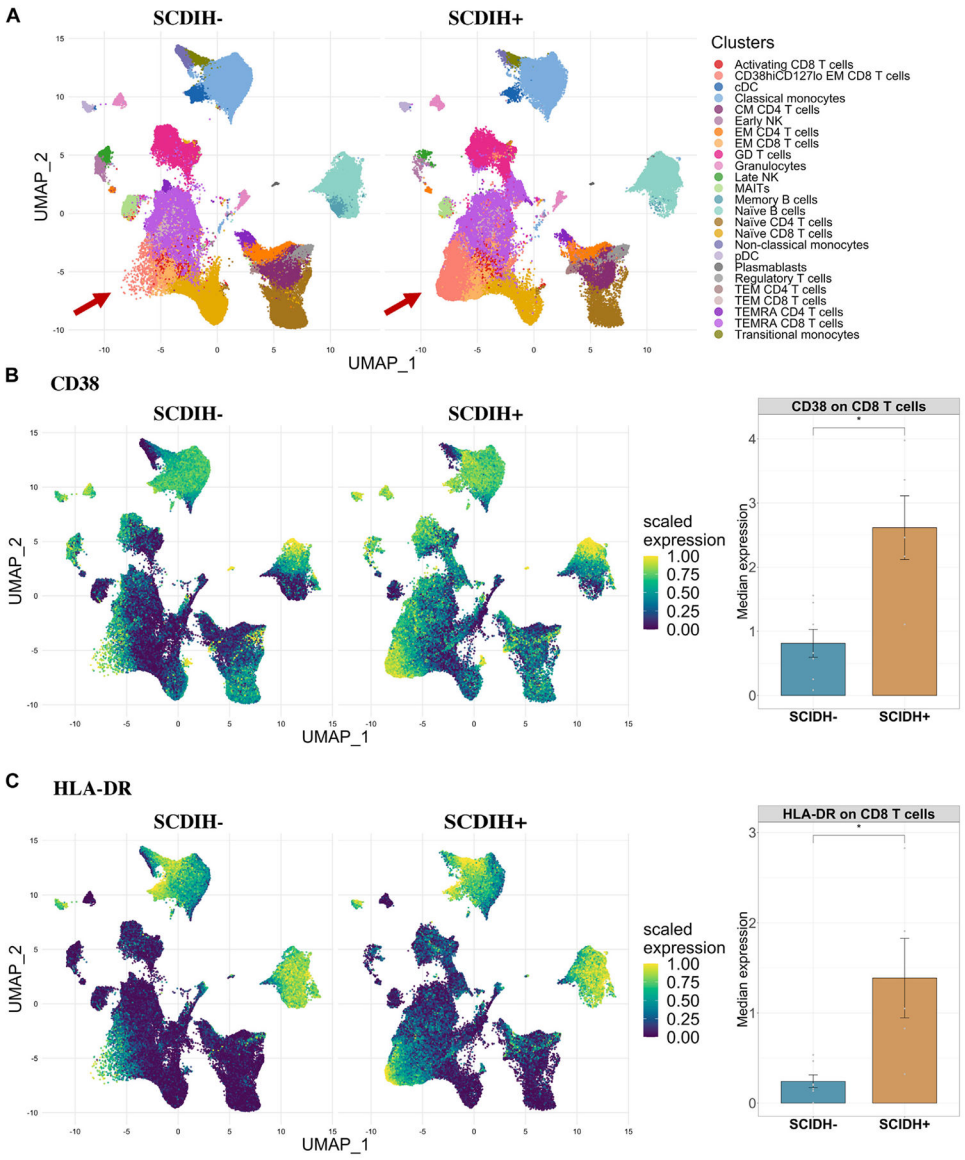

FIG 2.

CyTOF analysis of PBMCs from the patients in the SCIDH+ and SCIDH− groups revealed a skewed phenotype for $CD8^+$ T cells. **A**, A UMAP plot of cells after quality control, split by group, and colored according to the immune subsets identified after *FlowSOM and ConsensusClusterPlus* clustering (see this article's Materials section in the Online Repository at www.jacionline.org). **B**, Scaled expression of CD38 on PBMCs split by group and visualized as a UMAP plot and a histogram of median CD38 expression. **C**, Scaled expression of HLA-DR on PBMCs split by group visualized as a UMAP plot and a histogram of median HLA-DR expression. The Mann-Whitney-Wilcoxon test was used to compare the median expression of CD38 and HLA-DR in the SCIDH+ and SCIDH− groups. *cDC*, Classical dendritic cells; *CM*, central memory; *GD*, gamma-delta; *MAITs*, mucosal-associated invariant T-cells, *pDC*, plasmacytoid dendritic cells; *UMAP*, uniform manifold approximation and projection for dimensionality reduction. $*P < .05$.

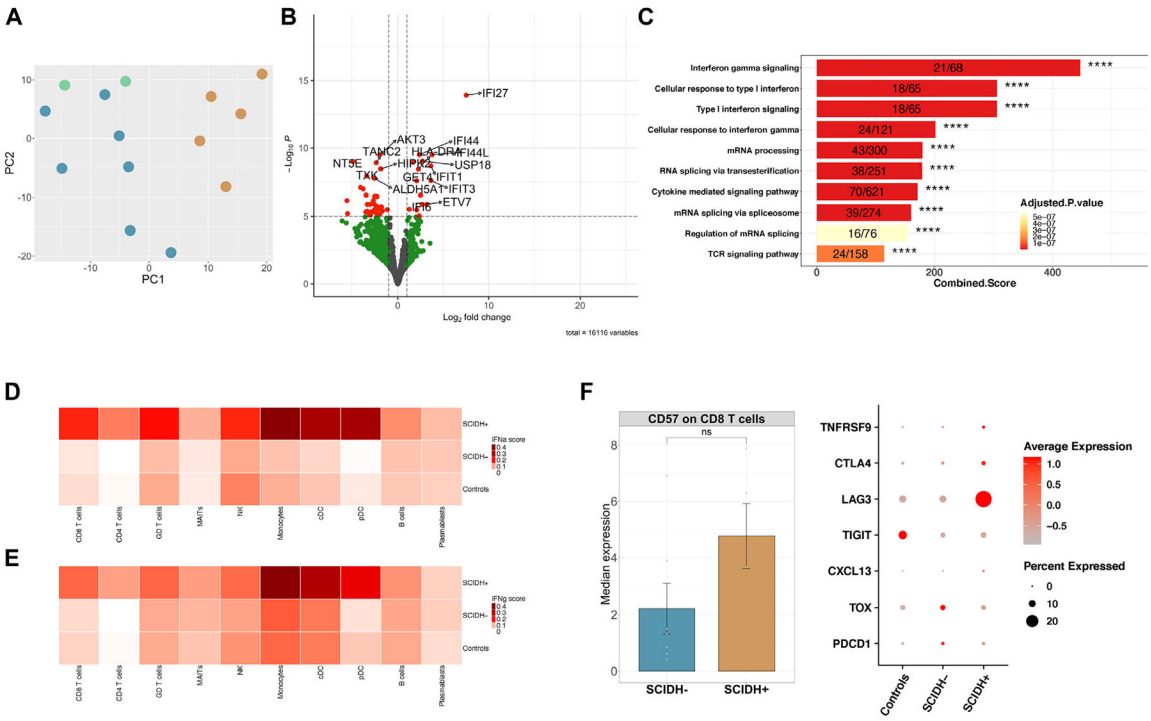

FIG 3.

scRNAseq analysis of PBMCs from patients in the SCIDH+ and SCIDH− groups and controls revealed an inflammatory CD8$^+$ T-cell phenotype and strong IFN signatures. **A**, A principal-component analysis of pseudo-bulk transcriptomic expression of CD8$^+$ T cells (green: controls; *blue*: SCIDH–; *brown:* SCIDH+). **B**, A volcano plot showing differentially expressed genes in CD8$^+$ T cells (pseudo-bulk expression). The *red dots* correspond to genes above both the fold change threshold and the *P* value threshold. **C**, A histogram of the results of a gene ontology analysis (GO Biological Process 2021) for upregulated genes in CD8$^+$ T cells from patients in the SCIDH+ group vs the SCIDH− group. **D** and **E**, A heatmap showing the mean of the module score for a published IFN-α response gene set (Fig 3, D) (MSigDB, Hallmark Interferon Alpha Response) and a published IFN-γ response gene set (Fig 3, E) (MSigDB, Hallmark Interferon Gamma Response) in each cluster, by group. **F**, A histogram showing the median expression of CD57 on CD8$^+$ T cells, as assessed by CyTOF (*left panel*), and a dot plot showing the mean expression and the proportions of CD8$^+$ T cells expressing the mentioned genes (scRNAseq, *right panel*) in samples from patients in the SCIDH+ and SCIDH− groups and controls. *cDC*, Classical dendritic cells; *CM*, central memory; *CTLA-4*, cytotoxic T lymphocyte–associated antigen 4; *CXCL13*, Chemokine (C-X-C motif) ligand 13; GD, gamma-delta; *MAITs*, mucosal-associated invariant T-cells; *pDC*, plasmacytoid dendritic cells; TIGIT, T-cell immunoreceptor with Ig and *ITIM* domain; *UMAP*, uniform manifold approximation and projection.

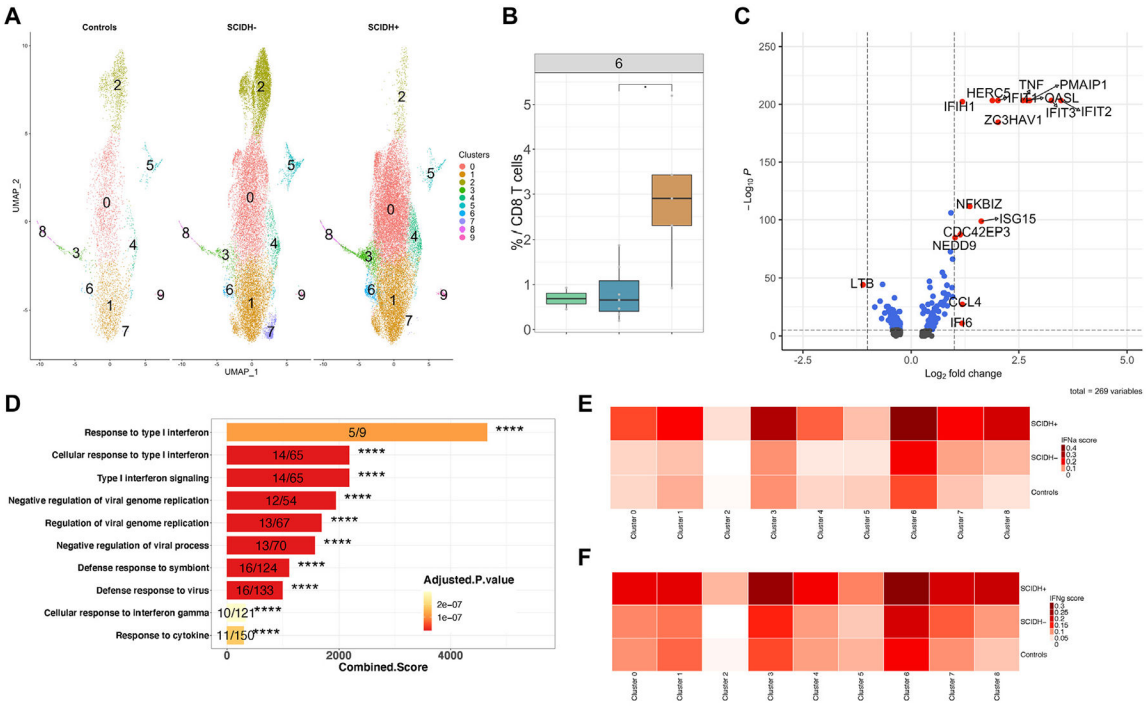

FIG 4.

Subclustering of CD8$^+$ T cells enabled the identification of an ISG^{high} CD8$^+$ T-cell cluster in the SCIDH+ group. **A**, A UMAP plot of CD8$^+$ T cells subclustered from PBMCs. **B**, A boxplot showing the proportion of CD8$^+$ T cells in cluster 6. **C**, A volcano plot showing upregulated and downregulated genes from cluster 6 (marker genes) vs all CD8$^+$ T cells, as assessed by the Seurat *FindMarkers* function. **D**, A histogram showing the results of a gene ontology analysis (using GO Biological Process 2021 database and *EnrichR*) for marker genes in cluster 6. The top 10 enriched pathways are shown and ranked according to their combined score. **E** and **F**, A heatmap showing the mean of the module score for a published IFN-α response gene set (Fig 4, E) and for a published IFN-γ response gene set (Fig 4, F) in each cluster of CD8$^+$ T cells separated by group. *UMAP*, Uniform manifold approximation and projection.

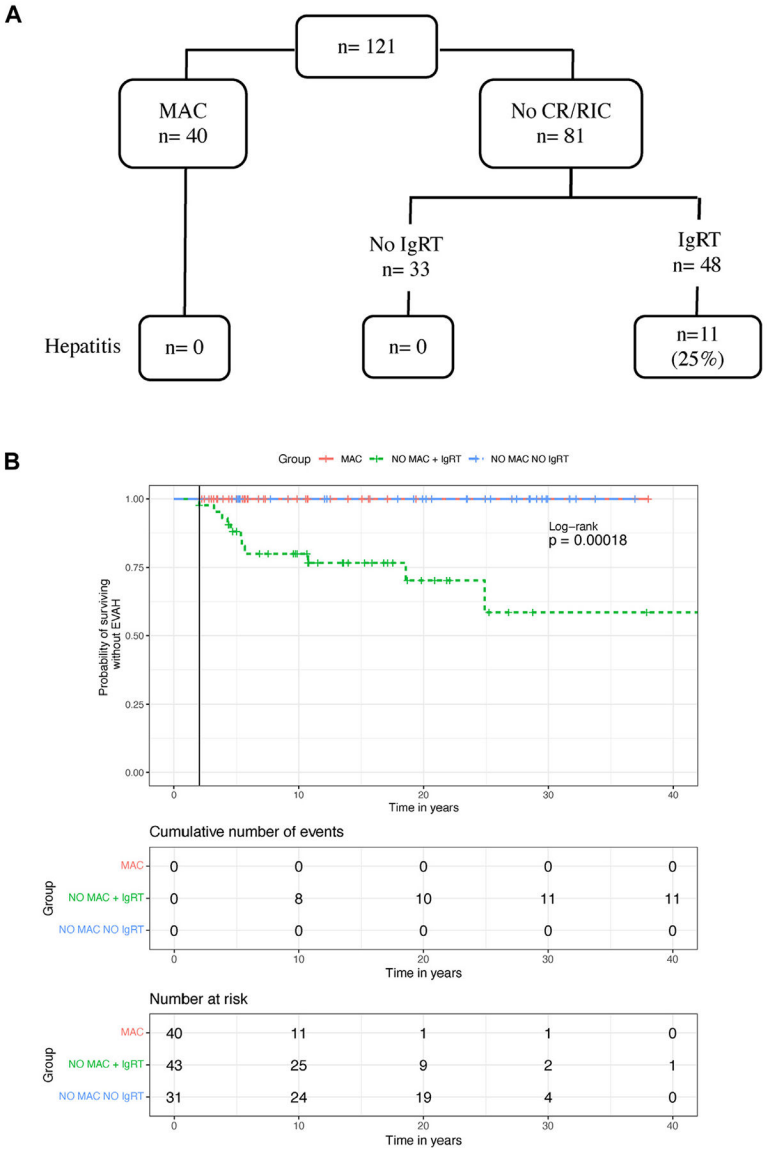

FIG 5.

Frequency and risk factors of hepatitis. **A**, A classification and regression tree analysis of the variables that best predicted the development of hepatitis. **B**, The cumulative probability of survival without developing hepatitis for the cohort. The vertical line indicates 2 years. *MAC*, Myeloablative conditioning; *RIC*, reduced-intensity conditioning (oral busulfan 8 mg/kg and cyclophosphamide 200 mg/kg only).

Table I.

Description of the index cases

	P1	P2	P3	P4	P5	P6	P7	P8	P9	P10	P11
Molecular diagnosis	IL-2Rγ	IL-2Rγ	IL-2Rγ	IL-2Rγ	IL-2Rγ	IL-2Rγ	DCLRE1C	IL-2Rγ	IL-2Rγ	IL-2Rγ	IL-2Rγ
Cellular therapy	HSCT	HSCT	HSCT	HSCT	HSCT	GT	HSCT	HSCT	HSCT	HSCT	HSCT
No. of cellular therapies	1	2	1	1	1	1	1	1	1	1	2
Age at cellular therapy (mo)	4	7/13	8	2.5	7	5.5	6.5	2.5	7	6.5	5
Donor	Haplo-id	Haplo-id	Haplo-id	Haplo-id	Geno-id	Autologous	Haplo-id	Haplo-id	Haplo-id	Haplo-id	Haplo-id
CR	ATG	ATG	ATG	ATG	0	Fludarabine *	Edx100	None	Bu8-Edx200	None	None/ bu8-Edx200
Age at last follow-up (y)	16	14.3	12.7	9.3	8.3	11	25	38	33	7	12
IgRT	+	+	+	+	+	+	+	+	+	+	+
Age hepatitis (y)	6	5	7.5	5.3	3.9	8.3	6	25	25	3	8
Other organs involved	Skin, spleen †	—	—	Skin	—	Spleen	Kidney, gut	Skin	—	Gut	Gut
Failure to thrive	+	+	+	+	+	−	+	−	−	+	+
Chronic diarrhea	+	−	−	−	+	−	+	−	−	+	+
Lobular hepatitis	+	+	+	+	+	+	+	+	+	+	+
Granuloma	+	−	−	+	−	−	+	+	+	−	+
RNH	+	+	+	−	−	+	+	+	−	−	−
TCR Vβ repertoire	Oligoclonal	Clones/ polyclonal ‡	Clones/ polyclonal ‡	ND	Clones/ polyclonal ‡	Clones/ polyclonal	Oligoclonal	Oligoclonal (liver)	ND	ND	ND
Virus on biopsies	AiV1	NoVII	—	—	ND	AiV1	AiV1	—	ND	Norovirus	—
Stools multiplex	SapoV	NoVII	NoVII	NoVII	SapoV		ND	ND	ND	Norovirus	ND

J Allergy Clin Immunol. Author manuscript; available in PMC 2023 December 01.

	P1	P2	P3	P4	P5	P6	P7	P8	P9	P10	P11
viral screening											
Treatment of hepatitis	Steroids,§ rapamycine, abatacept, ruxolitinib,§ infliximab	Ruxolitinib	Valganciclovir	None	FK-506,§ steroids§	Rapamycine§	Ciclosporine, rapamycine, steroids, infliximab, high-dose IgIV, TPN	Hydroxychloroquine IFN-*α*, infliximab, thalidomide	Ciclosporine	Steroids, rapamycine, TPN	Steroids
Donor chimerism	T, 100%; M, 0%	T, 100%; M, 0%	T, 100%; M, 0%	T, 100%; M, 21%//	T, 97%; M, 1%	NA	T, 100%; M, 0% D	T, 100%; M, 0% D	T, 100%; M, 0% D	T, 100%; M, 0% D	T, 100%; M, 0% D
Outcome	GT, cured	GT, cured	GT, cured	HSCT, cured	Spontaneous improvement	HSCT, early follow-up	Death	HSCT, cured	Alive	Death	Death

AiV, Human Aichi virus type 1; *ATG*, anti-thymocyte globulin; *D*, donor; *ND*, not done; *NoV II*, norovirus type II; *haplo-id*, haplo-identical transplant; *P*, patients; *RNH*, regenerative nodular hyperplasia; *SapoV*, sapovirus; *TPN*, total parrenteral nutrition; *bu8*, Busulfan 8 mg/kg; Edx200, 200 mg/kg; *T*, T-cells; *M*, myeloid cells.

*P6 underwent nonmyeloablative CR with fludarabine 2 × 40 mg/m^2 because of maternal T-cell expansion.

†Appearance of splenomegaly and thrombopenia.

‡The TCR Vβ repertoire displayed predominant clones and a polyclonal background.

§Treatment at the time of sampling for multiomics: low-dose ruxolitinb and steroids for P1, FK-506 and low-dose steroids for P5, rapamycine for P6, and nothing for P2, P3, and P4.

//P4: CD19 and NK-cell chimerism of 30% and 40%, respectively.